Physical Communication 68 (2025) 102579

Contents lists available at ScienceDirect

Physical Communication

journal homepage: www.elsevier.com/locate/phycom

Full length article

Noise removal techniques for underground communication systems based on matching pursuit

Yong Wang [a,b], Bangwei Yu [a,b], Ying Wang [a,b,*], Liangang Qi [a,b], Yang Liu [c]

[a] College of Information and Communication Engineering, Harbin Engineering University, Harbin 150001, China
[b] Key Laboratory of Advanced Ship Communication and Information Technology, Harbin Engineering University, Harbin 150001, China
[c] Sichuan Key Laboratory of Agile Intelligent Computing, Chengdu 610036, China

ARTICLE INFO

Keywords:
Underground communication systems
Pump noise
PIPOMP algorithm
Observation vector
Bit error rate

ABSTRACT

In underground communication systems, continuous mud pulse signals are susceptible to pump noise during transmission, resulting in a high bit error rate (BER). In this paper, a Paradigm Inner Product Orthogonal Matching Pursuit (PIPOMP) algorithm is proposed for the transmission characteristics of continuous waves in the underground. First, the observation vectors of pump noise are obtained by signal cyclic prefix (CP) differencing, and the resulting observation vectors are more accurate than the traditional methods. Second, the columns of the sensing matrix that are most relevant to the observation vectors are selected as candidate support sets by computing the L2 paradigm. Then, the least squares method was used to solve for the estimated value of the pump noise at the previous moment. Finally, the pump noise is reconstructed by combining the correspondence between the time and frequency domains. This paper establishes a complete underground communication system. We simulate the denoising performance of pump noise under stable and unstable conditions and analyze the denoising performance of the PIPOMP algorithm in depth. Simulation results show that the algorithm significantly improves the interference immunity performance and reduces the system BER in the environment where pump noise interferes and the fading is more drastic.

1. Introduction

Underground ultra-reliable and low-latency communications play a great role in oil exploration and development [1]. However, underground communication in the transmission process will be affected by some physical factors contain a lot of noise, the most significant of which is the pump noise [2]. With the increasingly harsh environment of oil exploration, the difficulty of exploration is increasing [3]. High-quality real-time downhole data is essential for operators [4]. In order to ensure the efficient work of oil exploration, the study of downhole wireless communication is very important [5]

Signal detection and noise removal techniques are key to the research of underground communication technology [5]. In 2017, Qu F et al. in the literature [6] utilized an adaptive noise cancellation method for dual pressure sensors to eliminate signal noise, and after field experiments it was obtained that the main components of the noise in the frequency domain were reduced by 49%–92%, which is seen to be unsatisfactory for noise removal; In 2019, S. M. Mwachaka et al. proposed adaptive time-domain noise suppression method for denoising in the literature [7], but it tends to cause attenuation of the communication signal energy, leading to severe signal distortion; In 2019, Zya B et al. used dual-sensor time-domain delay difference method for denoising in the literature [8], but it was significantly affected by the variation of noise characteristics, which resulted in less thorough noise removal; In 2020, Liang Y et al. proposed the use of wavelet transform to process the noise of high rate mud pulse signal in literature [9], but it is necessary to compare the correlation coefficients and reconstruction coefficients of the signals before and after denoising, and it is difficult to determine the optimal parameter combinations for the denoising process of mud pulse signal, and the denoising effect is poor; In 2021, ShiLong Cheng et al. in literature [10] designed low-pass filter to remove noise signals above 0.5 Hz, which can remove most of the noise, but the denoising effect is too poor; In 2022, Bo Yang et al. proposed a mud signal denoising network based on convolutional neural network in the literature [11], and the denoising effect was improved, but it was difficult to build the network and the operation was more difficult; In 2023, Simin Jiang proposed an improved constant center frequency modal decomposition algorithm based on the narrowband signal characteristics of pump

* Corresponding author at: College of Information and Communication Engineering, Harbin Engineering University, Harbin 150001, China.
E-mail addresses: wangyong@hrbeu.edu.cn (Y. Wang), yubangwei123@163.com (B. Yu), wangyingstu@163.com (Y. Wang), qiliangang@hrbeu.edu.cn (L. Qi).

https://doi.org/10.1016/j.phycom.2024.102579
Received 10 May 2024; Received in revised form 23 September 2024; Accepted 30 November 2024
Available online 7 December 2024

noise harmonics in literature [12], which has better performance in denoising, but the complexity is too high.

Compressed sensing technology is constantly evolving and plays an important role in different fields and shows better performance. In order to overcome the interference problem of pump noise, this paper uses the compressed sensing method to remove the pump noise. In this paper, we focus on analyzing the underground continuous wave transmission characteristics, building an underground complex channel model, and designing a scheme to eliminate the pump noise by using the compressed sensing reconstruction technique.

The main contributions are summarized as follows:

(1) In this paper, we propose a new method to compute the noise observation vector. First, adding the CP in front of the data. Then the CP of the current set of data received is made differential to the CP of the previous set of data. Finally the observation vector of the noise is obtained by period expansion.

(2) In this paper, a PIPOMP algorithm is proposed. We use the calculation of the inner product of L2 paradigm to select atoms, and the selected atoms are more relevant. Then, the estimate of the pump noise at the previous moment is solved by the least squares method. Finally, the pump noise is accurately reconstructed by the correspondence between the time and frequency domains, combined with the phase transform.

(3) This paper designs a complete underground communication system. We analyze the pump noise characteristics and simulate the complex channel environment using a time-varying channel model. The denoising performance is analyzed from two aspects.

2. System modeling

Single-carrier phase-modulated signals have high immunity to interference. When the phase is inherited, the noise immunity of the signal will be further improved [13]. Assume that the message signal $m(t)$ is composed of binary bits. Then the transmitted signal $s_{c.p.}(t)$ with phase inheritance can be expressed as:

$$\begin{aligned} s_{c.p.}(t) &= A_0 \sin\left(\omega_0 t + \theta - m(t)\right) \\ &= A_0 \sin\left(\omega_0 t + \theta - \sum_{n=1}^{n} \frac{4a_n+2b_n+c_n}{4} \Pi_{n,t}\right) \end{aligned} \tag{1}$$

Where A_0 denotes the signal amplitude, ω_0 denotes the carrier frequency, θ denotes the initial phase, and $a_n b_n c_n$ denotes the nth three-bit binary information bit.

$$\Pi_{n,t} = \frac{\pi}{2} + \frac{1}{T_0}\int_{-\infty}^{\infty} \frac{\sin\left(\frac{\omega T_0}{2}\right)}{\omega^2} \sin\left(\omega\left(t - 4nT_0 + \frac{7T_0}{2}\right)\right) d\omega \tag{2}$$

Where T_0 denotes the duration of the pulse. $s_{c.p.}(t)$ is transmitted through a fluid medium with severe amplitude attenuation to obtain a received signal $r(t)$, denoted as

$$r(t) = \int_{-\infty}^{\infty} s_{c.p.}(\tau)\, h(t-\tau) d\tau + n(t) + p(t) \tag{3}$$

Where $n(t)$ denotes additive Gaussian white noise and $p(t)$ denotes pump noise, see Section 3.1. $h(t)$ denotes the channel impulse response. Unlike terrestrial environments, there is more severe multipath fading of signals when transmitting signals using fluidic media [14]. Typically, the phase attenuation model of the received multipath signal is modeled using a uniform distribution obeying $(0, 2\pi)$. Therefore, $h(t)$ can be modeled as

$$h(t) = \sum_{k=0}^{L-1} a_k \delta\left(t - \tau_k\right) e^{j\theta_k} \tag{4}$$

Where L denotes the number of channel paths, a_k denotes the amplitude of the kth path, τ_k denotes the delay of the kth path, and θ_k denotes the phase of the kth path.

We can use the Nakagami distribution to approximate the multipath amplitude statistical model that simulates small-scale fading in the downhole environment. That is, the parameter a_k of Eq. (4) can be approximated by the Nakagami distribution with variable parameters. We model the delay characteristics of each path through a Poisson distribution. When discussing statistical modeling of multipath arrival times, the relative delay, expressed as $\left\{\tau_k - \tau_0\right\}_0^{L-1}$, is generally used. The received multipath signal phase statistics can be modeled as a uniform distribution obeying $(0, 2\pi)$.

According to Eqs. (1) and (2), we find that the carrier period in the code element inherits the phase of the over-period and is continuous and cumulative. Therefore, at the receiver side, we use phase demodulation. Fig. 1 shows the specific flow of phase demodulation. The codeword judgment is performed by phase difference. Note that we default the initial phase to 0. The phase judgment rule is expressed as

$$\begin{cases} 0 \le \Delta\varphi < \pi/8, & '000' \\ \pi/8 \le \Delta\varphi < 3\pi/8, & '001' \\ \vdots & \vdots \\ 11\pi/8 \le \Delta\varphi < 13\pi/8, & '110' \\ 13\pi/8 \le \Delta\varphi < 2\pi, & '111' \end{cases} \tag{5}$$

Using Eq. (5), we can determine the unit bit information carried by the code element and thus obtain all the bit data.

3. Noise detection & removal

Mud pulse signals are affected by a variety of noises during transmission, which mainly include Gaussian noise and pump noise. Gaussian noise can be filtered using equalization algorithms [15], pump noise is difficult to remove using traditional algorithms. Therefore, this paper focuses on algorithms to remove pump noise.

3.1. Pump noise characteristics

The pump noise $p(t)$ consists mainly of the fundamental wave and its higher harmonic signal components that are equal in frequency to the pump impulse signal. The pump noise can be expanded into the form of the sum of the fundamental and a number of harmonics by means of the Fourier transform [16], so that the pump noise can be modeled as

$$p(t) = \sum_{k=1}^{\infty} A_k \sin(2\pi f_k t + \theta_0) \tag{6}$$

Where, A_k denotes the amplitude of the kth harmonic, θ_0 denotes the initial phase, and f_k denotes the frequency of the kth harmonic. Its frequency can usually be calculated as

$$f_k = \frac{k \times F}{60} \tag{7}$$

Where F denotes the stroke rate and k denotes the number of times.

The triplex pump produces interference at a fundamental frequency of about 3.4 Hz, a second harmonic frequency of about 6.7 Hz, and a third harmonic frequency of about 10.2 Hz [16]. Pump noise interference consists mainly of the fundamental frequency and its second and third harmonics. The pump noise exhibits sparse characteristics in the frequency domain. Fig. 2 shows the time and frequency domain waveforms of the pump noise.

3.2. The denoising algorithm proposed in this paper

According to the analysis of the pump noise characteristics in the previous section, we can find that the pump noise shows sparse characteristics in the frequency domain. Therefore, noise removal can be performed by the algorithm of compressed sensing. For channel environments with more severe fading, the denoising performance of traditional compressed sensing algorithms is not satisfactory. In order to improve the accuracy of the received data and to reduce the BER

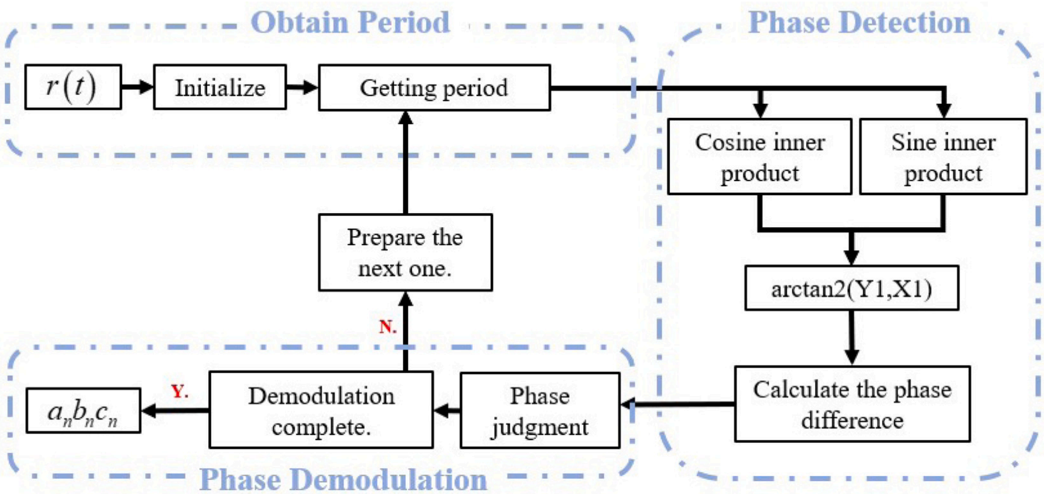

Fig. 1. Specific flow of phase demodulation. Where and denote the values of the inner product of the stabilized codeword period with the cochannel cosine and cochannel sine, respectively.

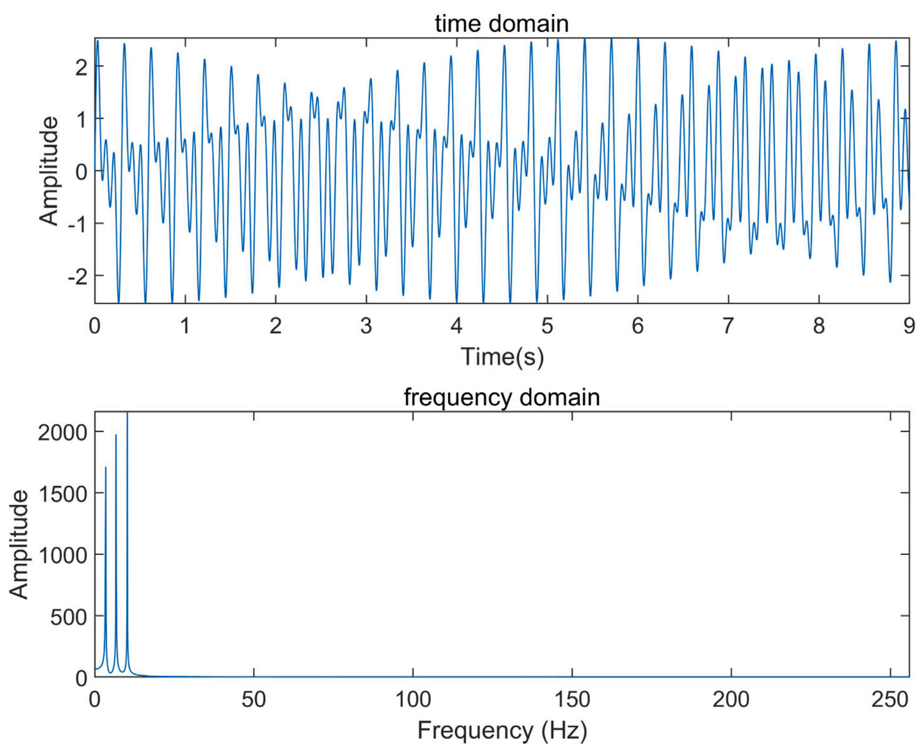

Fig. 2. Time and frequency domain waveforms of stabilized pump noise.

of the system, an improved compressive sensing denoising algorithm is proposed in this paper.

For a digital sampling system, we set the sampling frequency to f_s and the sampled discrete signal is denoted as $r(n)$. We can use $\boldsymbol{r}$ to denote the sampled signal vector. Because the communication system has a synchronization process, the carrier frequency of the signal can be known at the receiving end.

We unfold the received $N * 1$ time-discrete signal $\boldsymbol{r}$ under the orthogonal basis vector $\{\psi_i\}_{i=1}^{N}$ for processing. The sparse matrix $\boldsymbol{\psi} = [\psi_1, \psi_2, \dots \psi_N] \in R^{N\times N}$ is constructed by viewing $\{\psi_i\}_{i=1}^{N}$ as a column vector, then the signal $\boldsymbol{r}$ can be expressed as

$$\boldsymbol{r} = \sum_{i=1}^{N} \theta_i \psi_i \quad or \quad \boldsymbol{r} = \boldsymbol{\psi}\boldsymbol{\theta} \tag{8}$$

Where the constant coefficients are $\theta_i = \langle \boldsymbol{r}, \psi_i \rangle = \psi_i^T \boldsymbol{r}$. $\boldsymbol{\psi}$ is called the sparse matrix. In this paper the sparse matrix is obtained using discrete cosine transform. $\boldsymbol{\theta} = [\theta_1, \theta_2, \dots, \theta_N]^T \in R^{N\times 1}$ is called sparse coefficient vector and is obtained by Fourier transform.

We project the signal $\boldsymbol{r}$ with a measurement matrix $\boldsymbol{\Phi} \in R^{M\times N} (M \ll N)$ that is uncorrelated with the sparse matrix. Denoted as

$$\boldsymbol{y_p} = \boldsymbol{\Phi}\,\boldsymbol{r} = \boldsymbol{\Phi}\boldsymbol{\psi}\boldsymbol{\theta} = A\boldsymbol{\theta} \tag{9}$$

Where $\boldsymbol{y_p}$ is called the observation vector of noise, $A = \boldsymbol{\Phi}\boldsymbol{\psi}$ is called the sensing matrix.

The observation vector $\boldsymbol{y_p}$ of the noise, which we can obtain by time-differential measurement operations. Specifically, a CP is added to the end of the transmitted bit data. Then the CP data at the corresponding position in the received signal $\boldsymbol{r}$ is found. The observation vector of noise is finally obtained by making a difference between the CP of the current set of data and the CP of the previous set of data. Finally the observation vector of the noise is obtained. The length of the CP in this paper is the length of three bits of binary bit data. Because the pump noise is cyclic, we can get the pump noise data with the same length of the signal by cycle expansion. Note that, $\boldsymbol{y_p}$ are both period-expanded noisy observation vectors.

It can be seen from the above analysis. The pump noise can be recovered by using the obtained observation vector $\boldsymbol{y_p}$, sensing matrix A and sparsity K as inputs to the compressed sensing reconstruction algorithm. Therefore, based on the theory of compressed sensing, this paper proposes a PIPOMP algorithm. We choose atoms by computing a form of L2 paradigm. Finding the t columns in the sensing matrix A that are most relevant in the observation vector $\boldsymbol{y_p}$. Finally, these columns are used as candidate support sets.

We can obtain an $N * 1$ matrix B by multiplying the unit array P by each column of A. We can find the L2 paradigm of matrix B as follows:

$$\|B\|_2 = \sqrt{B(1,1) + B(2,1) + \cdots + B(N,1)} \tag{10}$$

Where, $B(N,1)$ denotes the Nth row, first column of matrix B.

Then the normalization calculation is performed. Finally, the residual r_0 is multiplied with the normalized result and the absolute value is taken to obtain the atomic candidate support set. The detailed steps of the PIPOMP algorithm are given by Algorithm. 1.

Algorithm 1: PIPOMP reconstruction algorithm.

Input: $\boldsymbol{y_p}$: observation vector of pump noise, A : sensing matrix, K : sparsity.

Output: $\Delta\hat{e}_p$: reconstructed noise, r_t : residual.

1. Initialization:Number of iterations $t = 1$, initial residuals $r_0 = \boldsymbol{y_p}$, initial index set $\Lambda_0 = \phi$, initial atomic support set $A_0 = \phi$.
2. Calculate the correlation of each column of the matrix A with the vector r_0. Multiply the unit array P by each column of A. Calculate the L2 paradigm number of the correlated columns and normalize $PA_{2-norm} \leftarrow (P * A_j)./\left\|P * A_j\right\|_2$, multiply the residuals r_0 by the normalized result and take the absolute value $beta_j \leftarrow |{r_0}^T * PA_{2-norm}|$.
3. Sort the results of $beta$ in step 2 to find the largest t columns and form the set J_t (the set of column order numbers) from these column vectors;
4. Perform atom set and index set updates: $\Lambda_t = \Lambda_{t-1} \cup J_t$, $A_t = A_{t-1} \cup a_{J_t}$.
5. Solve for $\Delta\hat{e}_{pt}$ by least squares: $\Delta\hat{e}_{pt} = \arg\min \left\|y_p - A_t \Delta e_{pt}\right\| = (A_t^T A_t)^{-1} A_t^T \boldsymbol{y_p}$.
6. Update the current residuals: $r_t = \boldsymbol{y_p} - A_t \Delta\hat{e}_{pt} = \boldsymbol{y_p} - A_t (A_t^T A_t)^{-1} A_t^T \boldsymbol{y_p}$.
7. Let the number of times $t = t + 1$, return to step 2 for the next iteration.
8. Judge the stop condition, if $norm(r_t) < 1e-6$ or $t > K$, then jump out of the loop.
9. The final estimate of the noise $\Delta\hat{e}_p$ is the last calculated $\Delta\hat{e}_{pt}$, $\Delta\hat{e}_p = \Delta\hat{e}_{pt}$.

We combine the correspondence between the time and frequency domains and write the output $\Delta\hat{e}_p$ of Algorithm. 1 as:

$$\Delta\hat{e}_p = \hat{e}_p - \hat{e}_{pX} = (1 - \exp(j2\pi\alpha))\,\hat{e}_p \tag{11}$$

Where $\hat{e}_p$ denotes the pump noise data of the previous moment. $\hat{e}_{pX}$ denotes the pump noise data of the current moment. α denotes the phase difference, which can be obtained from the phase change after modulation.

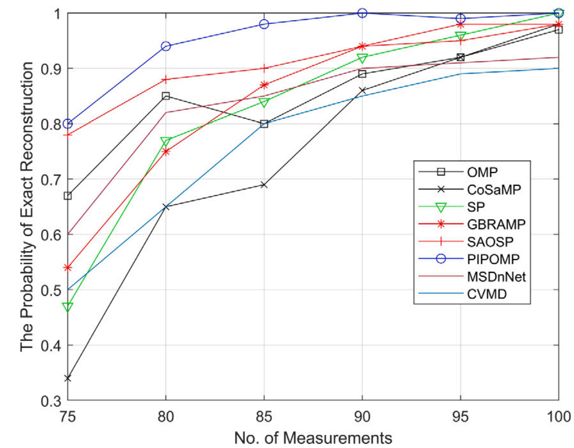

Fig. 3. Reconstruction rate with different observation vectors.

Finally, we can successfully solve for the pump noise $\hat{e}_{pX}$ according to Eq. (11). we subtract the pump noise $\hat{e}_{pX}$ from $\boldsymbol{r}$ of the received signal vector to obtain the complete signal. Then the bit signal is recovered by phase demodulation.

4. Numerical analysis

In this section, we numerically analyze the proposed denoising algorithm. To verify the reconstruction performance of the algorithms in this paper, this experiment compares the Orthogonal Matching Pursuit (OMP) algorithm [17], Compressive Sampling Matching Pursuit (CoSaMP) algorithm [18], Subspace Pursuit (SP) algorithm [19], Generalized Backtracking Regularized Adaptive Matching Pursuit (GBRAMP) algorithm [20], Sparse Adaptive Orthogonal Subspace Pursuit (SAOSP) algorithm [21], Mud Signal Denoising Net (MSDnNet) [11] and Constant center frequency Variational Mode Decomposition (CVMD) [12].

4.1. Reconfiguration success rate

We measure whether the reconstruction is accurate or not by the mean square error (MSE). We consider the reconstruction successful when the accuracy of the reconstruction is less than 10^{-6}. Where the mean square error can be expressed by the following equation.

$$\mathrm{MSE} = \frac{1}{n} \sum_{i=1}^{n} \left(x_i - \hat{x}_i\right)^2 \tag{12}$$

where x_i is the true value, $\hat{x}_i$ is the reconstructed value, and n is the total number of data points.

The length of the one-dimensional random signal selected for this experiment is 1256, and the number of trials is 100, and we stipulate that the reconstruction is successful if the reconstruction error is less than 10^{-6}. Fig. 3 shows the measurement results when the sparsity $K = 15$ and the observation vector is $[75, 100]$. Fig. 4 shows the measurement results when the observation vector is 70 and the sparsity is $[6, 30]$. Fig. 3 shows that the proposed algorithm in this paper is better with higher reconstruction rate for different observation vectors. Fig. 4 shows that at different sparsities, the algorithm proposed in this paper has a higher reconstruction rate when the sparsity is small, and the reconstruction performance is slightly lower than that of the OMP algorithm only near the sparsity $K = 20$. Considering the nature of the pump noise in this paper, the sparsity tends to be small, so it does not affect the reconstruction performance.When the observation vector is small or sparsity is large, the system is unsolvable and cannot be reconstructed out of the pump noise.

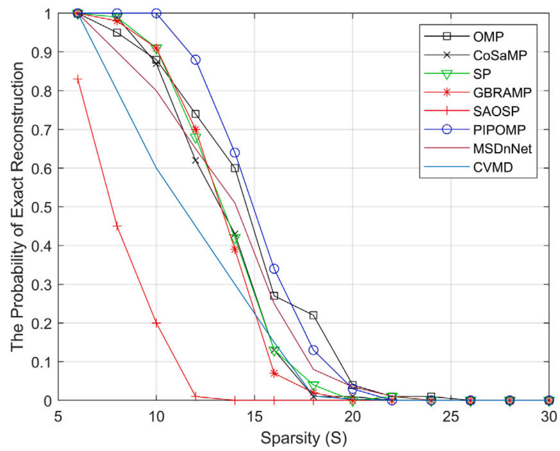

Fig. 4. Reconstruction rate at different sparsities.

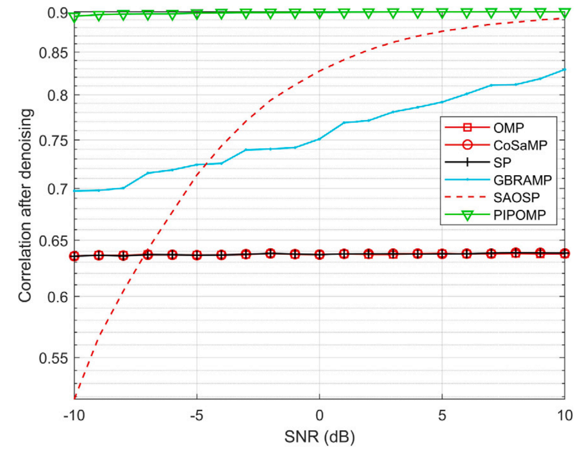

Fig. 5. Comparison of correlation coefficients after denoising when pump noise is stabilized.

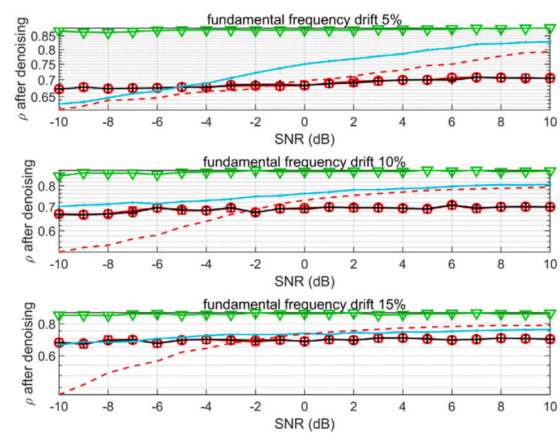

Fig. 6. Comparison of correlation coefficients after denoising at fundamental frequency drift of pump noise.

4.2. Correlation coefficient after denoising

In this paper the carrier frequency is 16 Hz, the carrier period is 1/16, and the sampling frequency is 32 Hz. The number of binary bits sent by the transmitter is 120 Bit.The total number of paths in the original downhole channel is set to 256, of which there are 10 major paths. The parameter g of the Nakagami distribution was set to 2. Doppler shift is zero [22]. The observation vector is selected to be 30% of the signal length. The sparsity of the pump noise $K = 3$. Each set of experiments is averaged over 500 runs.

The expression for the denoising correlation coefficient (ρ) is given by

$$\rho = \frac{\sum_{i=1}^{N} \hat{x}(i)x(i)}{\sqrt{\sum_{i=1}^{N} \hat{x}^2(i) \sum_{i=1}^{N} x^2(i)}} \tag{13}$$

Where ρ denotes the similarity between the reconstructed signal and the original signal, and its value ranges from $[-1, 1]$. The closer ρ is to 1, the greater the similarity.

The stabilizing pump noise is characterized as presented in Section 3.1. In order to better validate the performance of the denoising algorithm, we verified both the correlation coefficient and the system BER after denoising. When the Signal to Noise Ratio(SNR) is −10 dB, the correlation coefficient after denoising of the PIPOMP algorithm proposed in this paper is 0.8944. Eq. (5) shows that the correlation coefficient of the PIPOMP algorithm is the largest compared to the other algorithms, with the strongest correlation and the best noise removal.

The time and frequency domain characteristics of unstable pump noise are complex and usually manifest themselves in fundamental frequency drift and amplitude fluctuations [22]. The following three aspects are discussed below.

(1) Only fundamental frequency drift.

Under normal operating conditions, piston pumps may fluctuate their frequency slightly during operation, which may result in a shift in the fundamental frequency of the pump noise. Assuming a constant amplitude, the fundamental frequency fluctuates sinusoidally over a range of ±5%, ±10%, and ±15%. As in Fig. 6, the specific representation algorithm for each line remains consistent with Fig. 5. The correlation coefficient after denoising of the PIPOMP algorithm proposed in this paper is 0.8681 when the SNR is −10 dB and the fundamental frequency fluctuates by ±15%. In Fig. 6, the correlation coefficient after denoising of the PIPOMP algorithm proposed in this paper is significantly higher than that of other algorithms, so the correlation is stronger and the denoising effect is better.

(2) Only fundamental amplitude fluctuation.

The fundamental frequency of the pump noise is assumed to remain stable so that its amplitude fluctuates randomly within ±5%, ±10% and ±15%. As in Fig. 7, the specific representation algorithm for each line remains consistent with Fig. 5. The correlation coefficient after denoising of the PIPOMP algorithm proposed in this paper is 0.8452 when the SNR is −10 dB and the amplitude fluctuates by ±15%. In Fig. 7, the correlation coefficient after denoising of the PIPOMP algorithm proposed in this paper is significantly higher than that of other algorithms, and the advantage is more obvious at low SNR.

(3) Simultaneous variation of fundamental frequency and amplitude.

When the fundamental frequency and amplitude of the pump noise change at the same time, we assume that the fundamental frequency and amplitude of the pump noise fluctuate within ±10% at the same time. In such a complex situation, the PIPOMP algorithm proposed in this paper still performs well. As shown in Fig. 8, the correlation coefficient after denoising can be improved to 0.8430 when the SNR intensity is as high as −10 dB. By comparing the different curves, we can more clearly observe the advantages of the denoising performance of the PIPOMP algorithm.

In underground communication, pump noise has a great impact on existing algorithms, leading to their poor denoising results. Therefore, it is difficult for existing algorithms to overcome the effect of pump noise. The algorithm proposed in this paper starts from the characteristics of pump noise and obtains the observation vector of pump noise by means of cyclic prefix. The observation vector obtained by this

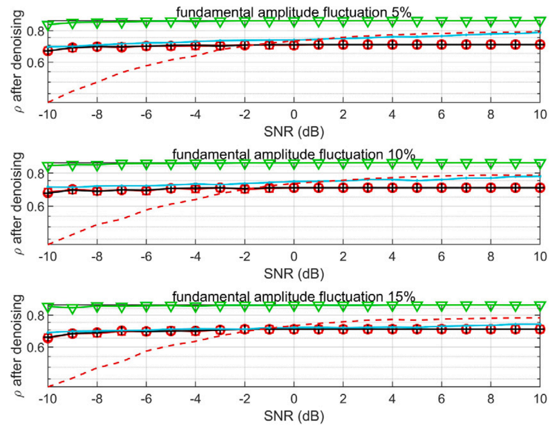

Fig. 7. Comparison of correlation coefficients after denoising for fluctuating pump noise amplitude.

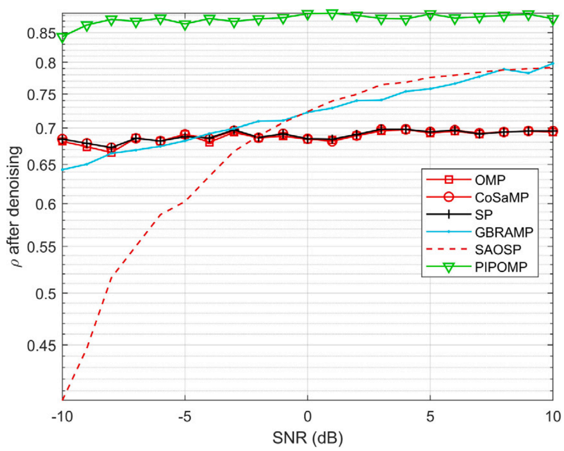

Fig. 8. Comparison of correlation coefficients after denoising for simultaneous changes in fundamental frequency and amplitude of pump noise.

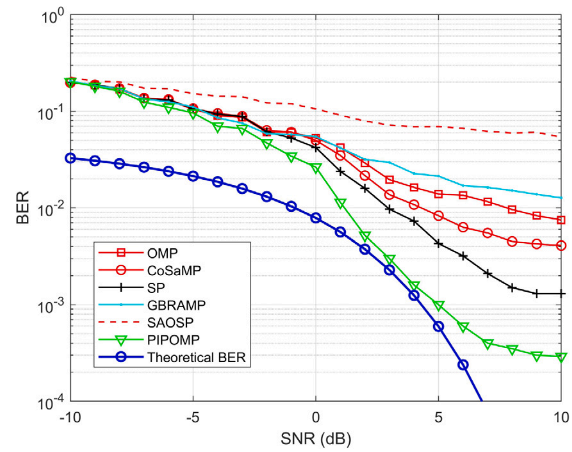

Fig. 9. Comparison of BER with stabilized pump noise.

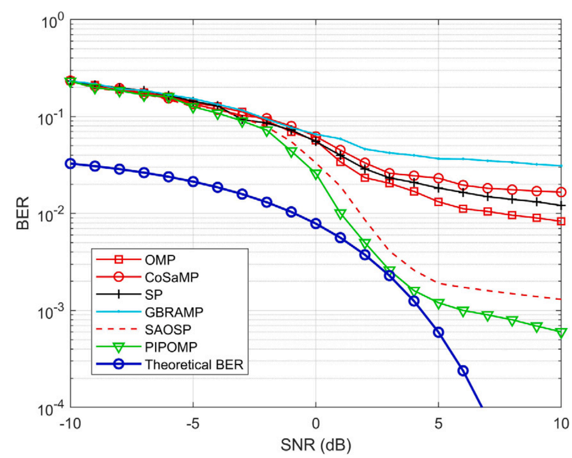

Fig. 10. Comparison of BER for simultaneous fluctuation of pump noise fundamental frequency and amplitude at ±10%.

method has stronger correlation and better removal effect on pump noise. The underground communication system in this paper adopts the coding method and equalization algorithm with better noise resistance. Therefore, the proposed algorithm is almost unaffected by SNR.

4.3. System BER

The theoretical BER formula for continuous wave 8PSK modulation is [23]

$$\hat{P}_e = erfc(\sqrt{SNR}\sin\frac{\pi}{8}) \tag{14}$$

Since pump noise exists at multiple frequencies, this affects the result of phase judgment. Eventually, this will lead to the occurrence of erroneous codes, which in turn will affect the BER performance of the system. To increase the persuasiveness of the proposed algorithm, in this section we add BER experiments. We simulated the stabilized pump noise and the pump noise fundamental frequency and amplitude when they fluctuated simultaneously at ±10%. The expression for the system BER is

$$Pe = Ne/N \tag{15}$$

Where N is the total number of binary codewords transmitted and Ne is the number of codewords that were transmitted in error.

Fig. 9 shows the system BER curve for stabilized pump noise. Fig. 10 shows the system BER curve for pump noise with both fundamental frequency and amplitude fluctuating at ±10%. Based on the BER curves in Fig. 9 and Fig. 10, it can be seen that the proposed algorithm in this paper has a slight performance advantage over the conventional reconstruction algorithm when the SNR is negative. However, when SNR is positive, the algorithm proposed in this paper performs significantly better and the system BER is lower.The algorithm proposed in this paper is suitable for SNRs of −5 dB and above, with little performance advantage at smaller SNRs. The proposed algorithm only simulates the real environment of underground oil exploration. Specifically, our solutions are suitable for gas phase, liquid phase, gas–liquid two-phase, and liquid–solid two-phase environments.

For complexity,we compare the complexity of different algorithms by analyzing the number of multiplication operations. We have compared the proposed algorithm with OMP algorithm, CoSaMP algorithm, SP algorithm, GBRAMP algorithm and SAOSP algorithm. As shown in Table 1. M is the dimension of the observation vector. N is the dimension of the sent data. K is the sparsity of the signal. We bring the parameters into Eq. The complexity of the PIPOMP algorithm proposed in this paper is 3×10^6, and the complexity of the OMP algorithm is 1.4×10^6. The performance of the PIPOMP algorithm is much higher than the OMP.

5. Conclusion

In this paper, we focus on the problem of continuous wave transmission process interfered by pump noise in complex channel environments, and we propose an improved compressive sensing reconstruction algorithm. First, we obtain the observation vectors by CP doing

Table 1
Complexity analysis of different algorithms.

Algorithm	Complexity
OMP	$O(K \times (M \times N + M \times K^2))$
CoSaMP	$O(K \log N \times (M \times N + M \times K^2))$
SP	$O(N^3)$
GBRAMP	$O(K \times (M \times N + M \times K^2))$
SAOSP	$O(K \times (M \times N^3 + M \times K^2))$
PIPOMP	$O(K \times (2 \times M \times N + M \times K^2))$

the difference, and the observation vectors obtained by this method are more strongly correlated with the pump noise. Then, the noise is reconstructed using the PIPOMP algorithm and finally the noise is removed. Through experimental simulations, we have analyzed the stable pump noise and unstable pump noise separately. We verified this in terms of the correlation coefficient after denoising and the system BER, respectively. The results show that the PIPOMP algorithm proposed in this paper has obvious advantages in denoising effect and reduces the system BER. This paper not only helps to solve the technical problems of deep oil and gas resources exploration and development, but also has a very wide application prospect. However, due to the more serious attenuation of underground communication signals, there is still some room for improvement of the denoising performance under low SNR conditions, and in-depth research will be carried out later.

CRediT authorship contribution statement

Yong Wang: Formal analysis, Data curation, Conceptualization. **Bangwei Yu:** Writing – original draft, Visualization, Validation, Project administration, Methodology. **Ying Wang:** Investigation, Funding acquisition. **Liangang Qi:** Validation, Supervision. **Yang Liu:** Resources, Project administration.

Declaration of competing interest

The authors declare that they have no known competing financial interests or personal relationships that could have appeared to influence the work reported in this paper.

Acknowledgments

This work is supported in part by Fundamental Research Funds for the Central Universities, China [3072022CF0801], National Key R&D Program, China [2018YFE0206500], and Sichuan Provincial Key Laboratory of Agile Intelligent Computing Project Fund.

Data availability

Data will be made available on request.

References

[1] Ying Wang, Qiang Guo, Jianhong Xiang, Linyu Wang, Yang Liu, Bi-orthogonality recovery and MIMO transmission for FBMC systems based on non-sinusoidal orthogonal transformation, Signal Process. (2024) 109427.
[2] Abbas Khaksar Manshad, Milad Ebrahimi Dastgerdi, Jagar A. Ali, Nazir Mafakheri, Alireza Keshavarz, Stefan Iglauer, Amir H. Mohammadi, Economic and productivity evaluation of different horizontal drilling scenarios: Middle East oil fields as case study, J. Petrol. Explor. Prod. Technol. 9 (2019) 2449–2460.
[3] Deli Gao, Some research advances in well engineering technology for unconventional hydrocarbon, Nat. Gas Ind. B 9 (1) (2022) 41–50.
[4] Mouhammed Jandal Berro, Matthias Reich, Laboratory investigations of a hybrid mud pulse telemetry (HMPT)–A new approach for speeding up the transmitting of MWD/LWD data in deep boreholes, J. Pet. Sci. Eng. 183 (2019) 106374.
[5] Saleh M. Mwachaka, Aiping Wu, Qingqing Fu, A review of mud pulse telemetry signal impairments modeling and suppression methods, J. Petrol. Explor. Prod. Technol. 9 (2019) 779–792.
[6] Fengzhong Qu, Zhujun Zhang, Junwei Hu, Jiangming Xu, Shiyuan Wang, Yezhou Wu, Adaptive dual-sensor noise cancellation method for continuous wave mud pulse telemetry, J. Pet. Sci. Eng. 162 (2018) 386–393.
[7] Saleh M. Mwachaka, Aiping Wu, Qingqing Fu, A review of mud pulse telemetry signal impairments modeling and suppression methods, J. Petrol. Explor. Prod. Technol. 9 (2019) 779–792.
[8] Zhidan Yan, Wenyi Xu, Chunwei Ai, Yanfeng Geng, Parametric study on pump noise processing method of continuous wave mud pulse signal based on dual-sensor, J. Pet. Sci. Eng. 178 (2019) 987–998.
[9] Yao Liang, Xiaodong Ju, Anzong Li, Chuanwei Li, Zhiping Dai, Li Ma, The process of high-data-rate mud pulse signal in logging while drilling system, Math. Probl. Eng. 2020 (2020) 1–11.
[10] ShiLong Cheng, Yule Hu, A novel signal processing algorithm for measurement while drilling (MWD) system, in: 2021 40th Chinese Control Conference, CCC, IEEE, 2021, pp. 3105–3109.
[11] Bo Yang, Wei Chen, Wenliang Wang, Guangming Guo, Noise modeling and deep learning noise suppression of mud signal, in: 2022 IEEE 17th Conference on Industrial Electronics and Applications, ICIEA, IEEE, 2022, pp. 1354–1359.
[12] Simin Jiang, Zhidan Yan, Ruirui Sun, Zuodan Wang, Hehui Sun, Study on signal decomposition-based pump noise cancellation method for continuous-wave mud pulse telemetry, Geoenergy Sci. Eng. 228 (2023) 211948.
[13] Changying Li, Huahai Qiu, Optimization algorithm and implementation of 8PSK modulation, in: International Conference on Communication and Electronic Information Engineering, CEIE 2016, Atlantis Press, 2016, pp. 400–405.
[14] Paul D. Panetta, Ultrasonic Characterization of Solid Liquid Suspensions, Technical Report, Pacific Northwest National Lab.(PNNL), Richland, WA (United States), 2010.
[15] Xin Zhang, Xiao-Ji Zhang, Xiao-Fei Xing, Li-Wei Jiang, Frequency domain response estimation of underwater acoustic channel and noise estimation for single-carrier frequency domain equalization, 2014.
[16] Zhidan Yan, Wenyi Xu, Chunwei Ai, Yanfeng Geng, Parametric study on pump noise processing method of continuous wave mud pulse signal based on dual-sensor, J. Pet. Sci. Eng. 178 (2019) 987–998.
[17] Joel A. Tropp, Anna C. Gilbert, Signal recovery from random measurements via orthogonal matching pursuit, IEEE Trans. Inform. Theory 53 (12) (2007) 4655–4666.
[18] D. Needell, J.A. Tropp, CoSaMP: Iterative Signal Recovery from Incomplete and Inaccurate Samples, (no. 12) Academic Press, 2008.
[19] Wei Dai, Olgica Milenkovic, Subspace pursuit for compressive sensing signal reconstruction, IEEE Trans. Inf. Theory 55 (5) (2009) 2230–2249.
[20] Mojisola Grace Asogbon, Yu Lu, Oluwarotimi Williams Samuel, Liwen Jing, Alice A. Miller, Guanglin Li, Kelvin K.L. Wong, GBRAMP: A generalized backtracking regularized adaptive matching pursuit algorithm for signal reconstruction, Comput. Electr. Eng. 92 (2021) 107189.
[21] Ying Wang, Qiang Guo, Jianhong Xiang, Yang Liu, Doubly selective channel estimation and equalization based on ICI/ISI mitigation for OQAM-FBMC systems, Phys. Commun. (2023) 102120.
[22] Guo Chen, Zhidan Yan, Tingzheng Gao, Hehui Sun, GuoLin Li, Junfei Wang, Study on model-based pump noise suppression method of mud pulse signal, J. Pet. Sci. Eng. 200 (2021) 108433.
[23] Seymour Stein, J. Jay Jones, Modern communication principles: with applications to digital signaling, 1967.

Yong Wang received M.S. and Ph.D. degrees from Harbin Engineering University in 2005 and 2011, respectively. Since 2005, he has been working at Harbin Engineering University. He is working as the academic team Membership of Harbin Engineering University on Communication System and Technology in Complex Electromagnetic Environment. His research interests include optical communication.

Bangwei Yu received his bachelor's degree in communications engineering from Harbin Institute of Technology in 2022. He is currently pursuing a master's degree in electronics and information at Harbin Engineering University. His research interests include digital signal processing, communication principles, 5G/6G wireless communications, orthogonal modulation schemes (e.g., OFDM), and massive MIMO.

Ying Wang received the B.S. degree in Communication Engineering from Henan College of Engineering in 2021. He is currently pursuing a Ph.D. in Information and Communication Engineering at Harbin Engineering University. His research interests are in signal processing, 5G/6G wireless communications, orthogonal modulation schemes (e.g., OFDM), non-orthogonal modulation schemes (e.g., FBMC), massive MIMO, etc.

Liangang Qi received the B.S. and Ph.D. degrees in information and communication engineering from Harbin Engineering University, China, in 2013 and 2018. He has been an associate professor at Harbin Engineering University since 2018. His research interests include electronic countermeasures, machine learning, radar target recognition, and radar signal processing.

Yang Liu received the Ph.D. degree in Signal and Information Processing from Southwest Jiaotong University in 2014. Since 2019, he has been working as a Senior Engineer at CLP 10 Research Institute. His recent research focus is on 5G/6G wireless transmission and waveform optimization.